Oxidative Dehydrogenation of Ethane over V_2O_5 (001): A Periodic Density Functional Theory Study

Guo-Liang Dai, Zhi-Pan Liu, Wen-Ning Wang,* Jing Lu, and Kang-Nian Fan*

Shanghai Key Laboratory of Molecular Catalysis and Innovative Materials, Department of Chemistry, Fudan University, Shanghai 200433, People's Republic of China

Received: July 25, 2007; In Final Form: October 11, 2007

Oxidative dehydrogenation (ODH) of ethane over the V_2O_5 (001) surface has been carried out using periodic density functional theory (DFT) calculations. We show that the first C−H bond activation leading to an ethoxide intermediate is the rate-limiting step of the reaction. The most feasible pathway for the C−H bond activation is predicted to take place at the O(1) (V═O) site, with activation energy of 35.1 kcal/mol. The O(2) (V−O−V) site is less active for C−H bond activation, with an energy barrier of 37.6 kcal/mol. However, the O(1) site exhibits much lower selectivity to ethene formation than O(2) because the side reaction leading to acetaldehyde occurs more easily than ethene production on O(1), whereas O(2) is inert for acetaldehyde formation. On the basis of our results, the ODH reactions of ethane and propane are systematically compared and discussed.

1. Introduction

The catalytic oxidation of light alkanes has been the subject of intensive studies because of its importance for the production of basic chemicals such as alkenes.[1−24] The oxidative dehydrogenation (ODH) of lower alkanes offers an attractive route to alkenes. One major advantage of the ODH reaction lies in the fact that it is thermodynamically favored at low temperatures, which would significantly reduce coke formation and extend the lifetime of catalysts.

Vanadium pentoxide (V_2O_5) is an important catalyst for the ODH reaction of light alkanes.[25−35] The ODH reactions over the vanadium-based catalysts have been extensively studied in the past decade, and the reaction mechanism originally proposed by Mars and van Krevelen has been accepted generally,[36−38] which can be described as (i) the reduction of the oxide surface by hydrocarbon and (ii) the subsequent reoxidation of the surface by the gas-phase oxygen. Mechanism studies on propane and ethane ODH reactions revealed that both reactions proceed via Mars−van Krevelen pathways involving lattice oxygen atoms,[2−4,39] and the first step in both propane and ethane oxidation reactions seems to involve the breaking of a C−H bond, which is regarded as the rate-limiting step.[40−43] Oyama et al.[3] investigated the ethane oxidation on V_2O_5/SiO_2 and 100% V_2O_5 samples. They found the main products of the reaction were acetaldehyde, ethene, CO, and CO_2, and the 100% V_2O_5 sample shows much lower activation energies. In addition, the 100% V_2O_5 sample prefer to produce extensively oxidized products throughout the entire temperature range. Comparing with the propane ODH reaction, the measured ODH rate of ethane is much lower.[35,44] This may be readily explained by considering that ethane consists of only a methyl C−H bond with a bonding energy of 420 kJ/mol while propane has two weaker methylene bonds (401 kJ/mol). However, the measured activation energies of ethane and propane are very similar,[35,44] and the origin of this remains unclear. One speculation is that the intermediate formed upon C−H bond activation of ethane is more stable than that of propane and thereby compensates for the C−H bond activity difference between these two molecules.[44]

In recent years, theoretical calculations, especially based on density functional theory (DFT), have been employed to study the mechanism of alkane ODH reactions over metal oxide catalysts. Both cluster and periodic slab models are adopted to model the catalytic system. The cluster model calculations of methane[42] and propane[43] ODH reactions over a Mo_3O_9 cluster demonstrated that the C−H bond activation of these two molecules share similar mechanisms and that the activation energies are generally higher for methane than those for propane. In these studies, the terminal oxygen (V═O) is considered to be the active site. In the cluster model study of propane ODH on V_2O_5, Redfern et al.[45] found similar energetics for the vanadyl V═O site and bridging V−O−V site, but the energy barriers for both C−H bond activation and propene formation are much higher than experimental observation. Periodic DFT study of propane ODH over a V_2O_5 (001) surface using a slab model obtained moderate energy barriers of C−H bond activation and propene formation comparable with experiments at both terminal V═O and bridging V−O−V sites, indicating that both lattice oxygen species may contribute to propane ODH.[46]

In this report, we present the first detailed periodic DFT study on the ethane ODH reaction over a V_2O_5 (001) surface. Various active sites and reaction mechanisms are examined. In addition to the reactions leading to ethene, other likely pathways leading to byproduct are also investigated. Similar activity of surface oxygen species and C−H bond activation mechanisms are found in ethane ODH as those in propane ODH. However, the energy barrier of C−H bond breaking for ethane is higher than that of propane, and the higher stability of reaction intermediate ethoxide on the surface than that of isopropoxide was not observed.

2. Computational Details

All total energy density functional theory calculations were carried out using the SIESTA package with numerical atomic

* To whom correspondence should be addressed. E-mail: wnwang@fudan.edu.cn; knfan@fudan.edu.cn.

10.1021/jp075843s CCC: $40.75
Published on Web 02/14/2008

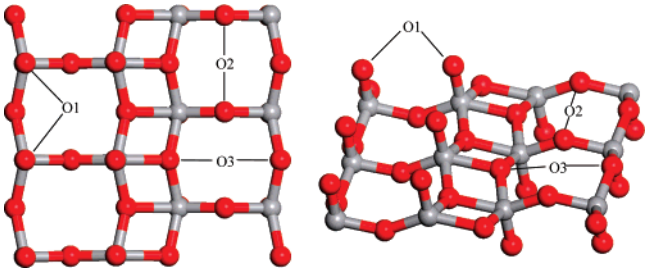

Figure 1. The unit cell of the V_2O_5 (001) surface.

orbital basis sets and Troullier−Martins normconserving pseudopotentials.[47,48] The exchange-correlation functional utilized is the generalized gradient approximation method, known as GGA-PBE.[49] A double-ξ plus polarization basis (DZP) set was employed. The orbital-confining cutoff radii were determined from an energy shift of 0.01 eV. The energy cutoff for the real space grid used to represent the density was set as 150 Ry. To further speed up calculations, the Kohn−Sham equations were solved by an iterative parallel diagonalization method that utilizes the ScaLAPACK subroutine pdsygvx with two-dimensional block cyclicly distributed matrix.[50] The Broyden method was employed for geometry relaxation until the maximal forces on each relaxed atom are less than 0.1 eV/Å. The V_2O_5 (001) surface is routinely modeled by a one-layer slab with all atoms allowed to relax. A (3×1) unit cell (11.54×10.81 Å) is used to model the surface and the vacuum region is 20 Å. Only the Γ-point was used to sample the Brillouin zone in our calculations. Spin-polarization was considered during all the calculations.

A constrained minimization scheme is employed to search the transition states (TSs) on the potential energy surface.[51,52] A TS is identified when (i) the forces on the atoms vanish and (ii) the energy is a maximum along the reaction coordinate but a minimum with respect to all of the other degrees of freedom. The energy barrier is determined as the energy difference between the saddle point and the initial state.

The adsorption energy (E_{ads}) is calculated as

$$E_{ads} = E(_{adsorbate-substrate}) - (E_{adsorbate} + E_{substrate})$$

where a negative E_{ads} indicates exothermic process.

3. Results and Discussion

3.1. Molecular Adsorption of Ethane. The molecular adsorption of ethane at various lattice oxygen sites on V_2O_5 (001) surface was first examined. It is found that the most stable adsorption structure is at the O(2) site with the adsorption energy only of −2.8 kcal/mol, showing that molecular ethane only physisorbs on V_2O_5 (001). For a comparison, the adsorption of propane on the surface of V_2O_5 (001) was also calculated. Similar to that of the ethane, the propane also has a physisorption state on the surface, with the adsorption energy of −2.5 kcal/mol and the most favorable adsorption site being at the O(2) site, in agreement with the previous report.[46] Considering that the ODH reaction occurs at high temperatures, e.g., ∼800 K, ethane in the gas phase is more stable than it is on the surface due to the large entropy contribution. It is thus expected that the C−H bond activation of ethane over V_2O_5 (001) is not precursor mediated.

3.2. C−H Bond Activation. Two different ways have been suggested as for how the C−H bond breaks on metal oxides.[53] One is heterolytic splitting, leading to an alkyl anion and a proton. The other is homolytic cleavage that usually takes place

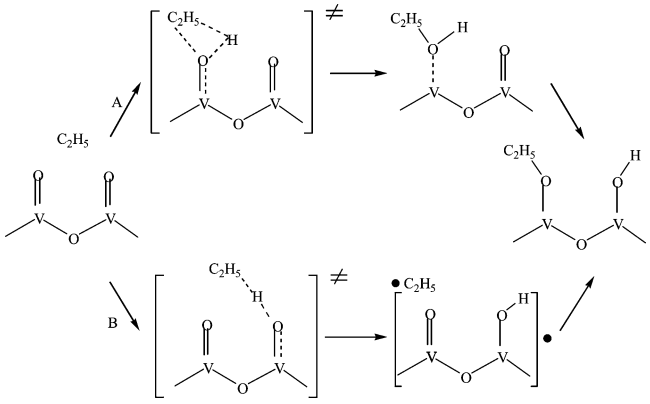

Figure 2. Homolytic cleavage mechanisms for the C−H bond activation of ethane.

at surface oxygen sites. For the ODH of propane, the previous study already showed that the chemical reaction of homolytic cleavage is more feasible.[46] The reaction follows two steps: (i) Propane dissociatively adsorbs on the surface to form a propoxide and a hydroxyl group. It is a process involving two lattice oxygen atoms. (ii) The propoxide then releases an H atom to a second lattice oxygen to produce propene. Therefore, for the ODH reaction of ethane, we consider the homolytic cleavage only, which can be represented as

$$C_2H_5{-}H_g + O_s{+}O_s \leftrightarrow C_2H_5O_s + HO_s$$

where g and s denote the gas phase and surface, respectively.

With three different types of lattice O on V_2O_5 (001) (Figure 1), nine possible combinations of two oxygen sites in total are available for the ODH reaction, i.e., O(1)-O(1), O(1)-O(2), O(1)-O(3), O(2)-O(1), O(2)-O(2), O(2)-O(3), O(3)-O(1), O(3)-O(2), and O(3)-O(3). According to our previous work on propane ODH reactions,[46] here we considered the two most favorable reaction mechanisms for each O-O combination, namely, the oxo-insertion mechanism (A) and the radical mechanism (B) (Figure 2). In mechanism A, a lattice oxygen atom inserts into the C−H bond of the ethane to form an ethoxide intermediate on the surface. The proton of the ethoxide is then transferred to another lattice oxygen nearby. For mechanism B, a lattice oxygen atom abstracts an H atom from ethane directly to leave an ethylic radical in the gas phase. It is then followed by the rebound of the ethylic radical to a second surface oxygen. In short, the C−H bond activation pathways can be denoted as O(m)-O(n)-X, where m, n = 1, 2, 3 and X = A, B, the first O(m) denotes the O site where an ethane attacks the surface initially. We will go through our DFT results for these pathways in the following subsections.

3.2.1. O(1) Site: O(1)-O(n)-X. (a) O(1)-O(n)-A. A terminal oxygen of V═O interacts with one of the ethane C−H bonds through the transition state TS1 to form a stable ethanol-like intermediate on the surface (Figure 3). The reaction barrier is 39.9 kcal/mol, and the relative energy of the products is about 2.2 kcal/mol with respect to the reactants. In TS1, the C−H bond is elongated from 1.12 Å of ethane to 2.06 Å, and the distance between the C atom of ethane and the O(1) atom is shortened to 2.71 Å. The length of O−H bond is 1.00 Å, indicating that the O−H bond is already formed at the same time. In the ethanol-like intermediate, the C−O bond and O−H bonds are formed with the bond length of 1.48 Å and 1.05 Å, and the C−H distance is now 2.14 Å. The subsequent migration of hydrogen to a nearby O(1) site can occur readily with an energy barrier of only 1.0 kcal/mol. This completes the O(1)-

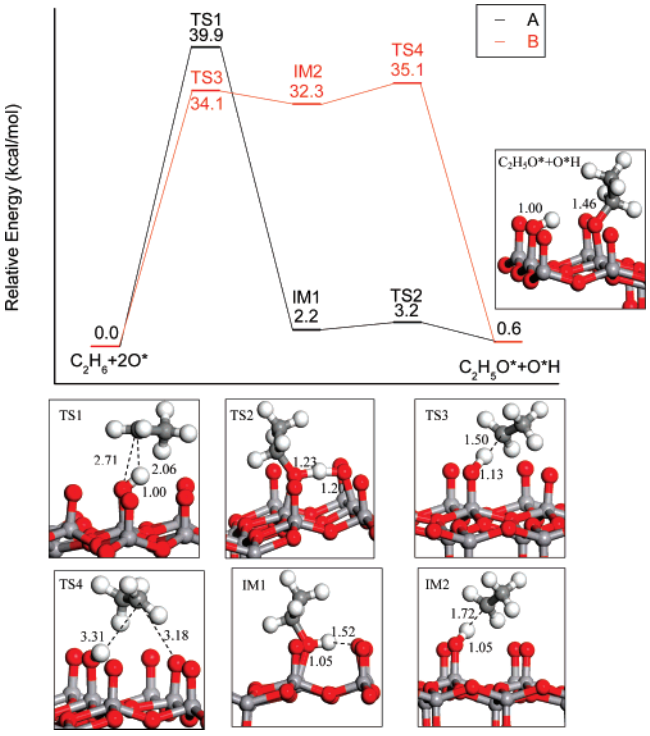

Figure 3. Energy profile of C−H bond activation at the O (1) site and the structures of related transition states and intermediates.

O(1)-A pathway. The final state of surface ethoxide is 0.6 kcal/mol less stable than the reactants.

As for the pathways of O(1)-O(2)-A and O(1)-O(3)-A, the reaction barriers required for the migration of the H atom to the nearby O(2) or O(3) sites are 18.0 kcal/mol and 20.8 kcal/mol, respectively. This is not surprising as the adsorption of H atom at O(2) or O(3) sites are less stable by 9.6 and 2.6 kcal/mol, respectively, than that at the O(1) site, Therefore, among the three O(1)-O(*n*)-A pathways, the O(1)-O(1)-A is the most feasible.

(b) O(1)-O(*n*)-B. For mechanism B, the H of ethane is abstracted by O(1) to form an ethyl radical in the gas phase. The energy barrier is calculated to be 34.1 kcal/mol, and the radical intermediate is only 1.8 kcal/mol more stable than the transition state (TS3). As shown in Figure 3, the C−H bond in TS3 is lengthened to 1.50 Å, and the O−H distance is only 1.13 Å, indicating the breaking of C−H bond and the formation of O−H bond. The radical intermediate may rebind with the nearby lattice O atoms in the next step. It is found that the rebinding of ethyl radical with the nearest O(1) site is the most feasible with a barrier of only 2.8 kcal/mol, while the energy barrier for that involving O(2) or O(3) is 5.5 or 7.3 kcal/mol, respectively. In addition, the ethoxide species on O(2) and O(3) are less stable than that on O(1). Obviously, O(1)-O(1)-B is the most favorable pathway among O(1)-O(*n*)-B pathways, and it is also energetically more feasible than O(1)-O(*n*)-A pathways.

The surface hydroxyl group on the O(1) site can also capture the H atom of ethane to form a water molecular and form an ethyl radical simultaneously, but the calculated energy barrier is as high as 40.4 kcal/mol. Therefore, compared with lattice oxygen O(1), the C−H bond activation by a surface hydroxyl such as O(1)-H is rather unlikely.

Comparing with the ODH reaction of propane at the O(1) site, we found that the activation of C−H bonds of these two alkanes follow the similar lowest energy pathway, namely, O(1)-O(1)-B, although the calculated energy barrier for ethane C−H bond activation is about 6.8 kcal/mol higher than that of propane.[46]

3.2.2. O(2) Site: O(2)-O(n)-X. The pathways of the O(2)-O(n)-X are similar with those of O(1)-O(n)-X in general. Here their main differences will be highlighted. For the insertion mechanism A, it is found that the energetically most favorable pathway at the O(2) site is O(2)-O(2)-A with the barrier of 37.6 kcal/mol. Because of the large distance between the O(1) and O(2) (Figure 1), the energy barrier of H atom migration in the pathway of O(2)-O(1)-A is as high as 50.4 kcal/mol. The binding of H atom with O(3) is the weakest on the surface. In the O(2)-O(3)-A pathway, the energy barrier required during the process of H atom migration is 2.9 kcal/mol higher than that of O(2)-O(2)-A (7.3 kcal/mol vs 4.4 kcal/mol).

In the radical mechanism, the activation energy of O(2)-O(n)-B pathways is at least 1.6 kcal/mol higher than that of O(2)-O(2)-A. Therefore, mechanism A is preferred to mechanism B over the O(2) site. Compared with the C−H bond activation on O(1) site, the energy barrier of the process taking place on the O(2) site is 2.5 kcal/mol higher (37.6 kcal/mol vs 35.1 kcal/mol). Obviously, the situation of C−H bond activation of ethane is very similar with the case of propane ODH. Both O(1) and O(2) sites are active for C−H bond activation with O(1) site slightly more active, and the most favorable reaction mechanism on these two sites are different.

3.2.3. O(3) Site: O(3)-O(n)-X. As reported in the previous study of propane ODH reactions,[53] the 3-fold coordinated O(3) is the most inert toward the C−H bond activation. Here two possible pathways are located on O(3), i. e. O(3)-O(3)-A and O(3)-O(1)-B, with high-energy barriers, of 46.9 and 42.2 kcal/mol, respectively. Moreover, the adsorption of ethoxide at O(3) will induce strong surface reconstruction by breaking one of the O(3)−V bonds. Therefore, as in the case of propane, the possibility of the 3-fold coordinated O(3) as the reaction center for ethane ODH reactions could be ruled out.

3.2.4. Electronic Structure Analysis. The changes of atomic charges of the system in the process of C−H bond activation were calculated by using Bader charge analysis, and the results of mechanism B on O(1) and O(2) sites were listed in Table 1 for comparison. Generally the results are very similar with those of the propane ODH reaction.[46] From ethane to ethoxide, two electrons are transferred to the surface. As the first step of C−H bond activation, one electron flows to the surface at TS3 and TS7. After that, upon ethyl radical rebonding with surface oxygen, another electron is transferred to the catalyst. It is notable that the injected electrons located on both vanadium and oxygen atoms. The delocalization of electrons on the surface accounts for the reactivity of oxygen sites with low reducibility, such as O(2). On the other hand, the vanadium atoms are not reduced as much as expected. The Bader spin-charge analysis also showed that the net spins are mainly located on the vanadium atoms directly linked to the reacting lattice oxygens. The strong spin polarization on V, which is mainly due to d-state, is expected to arise from the weakening of the original V−O d-p covalent bond resulting in the spin-polarized d-states on V.

3.3. Ethene Formation. From the adsorbed ethoxide, ethene can be produced by losing one of the H atoms of the methyl group to a nearby lattice oxygen. In the following, our results for the ethene formation from the ethoxide on the O(1) and O(2) sites will be presented in detail.

Starting from the ethoxide at O(1) site, its H atom of the methyl group can migrate to the nearby lattice O atoms,

TABLE 1: Bader Charge Differences of the Atoms in the System upon Going from the Initial State (ethane in the gas phase plus the clean surface) to the Transition States (TS), Intermediate States (IM), and Ethoxides on O(1) and O(2) Sites in the C−H Bond Activation[a]

	O(1)				O(2)			
	TS3	IM2	TS4	$C_2H_5O^*(1) + O^*(1)H$	TS7	IM4	TS8	$C_2H_5O^*(2) + O^*(2)H$
O(1)[b]	−0.21	−0.72	−0.74	−0.35				
O(2)[b]					−0.06	−0.61	−0.59	−0.60
V_{sum}[c]	−0.27	−0.23	−0.21	−0.25	−0.33	−0.36	−0.40	−0.72
O_{sum}[d]	−0.21	−0.38	−0.45	−1.08	−0.13	−0.36	−0.33	−0.30
C_2H_6	0.68	1.33	1.40	1.68	0.52	1.33	1.33	1.62
net spin (μ_B)	0.52	1.49	1.47	1.63	0.82	1.48	1.48	1.41

[a] Negative value means electron gain. The net spin of each state is also listed. The unit of Charge is|e|. [b] The reacting oxygen atoms in the unit cell. [c] Sum of the net charges on all V atoms in a unit cell. [d] Sum of the net charges on all O atoms in a unit cell except the reacting O atom.

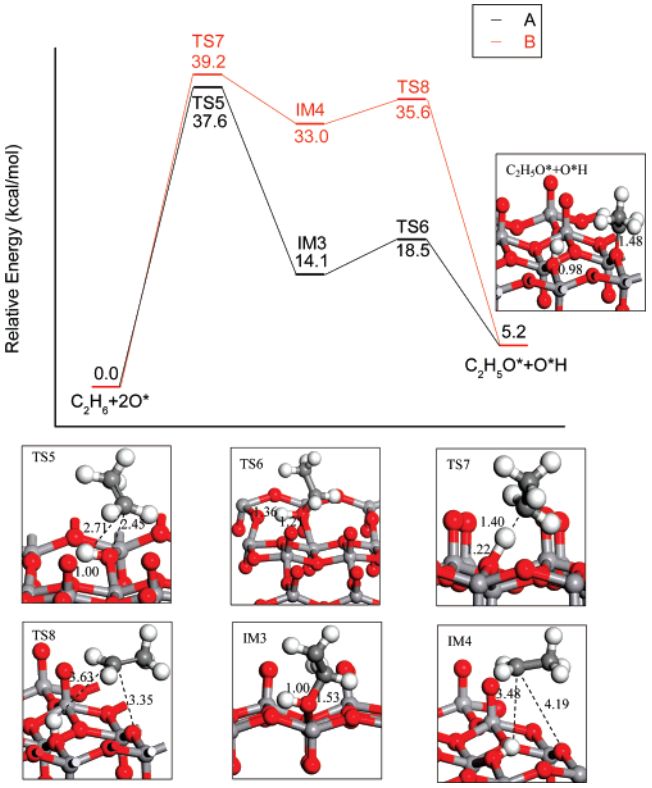

Figure 4. Energy profile of C−H bond activation at the O (2) site and the structures of related transition states and intermediates.

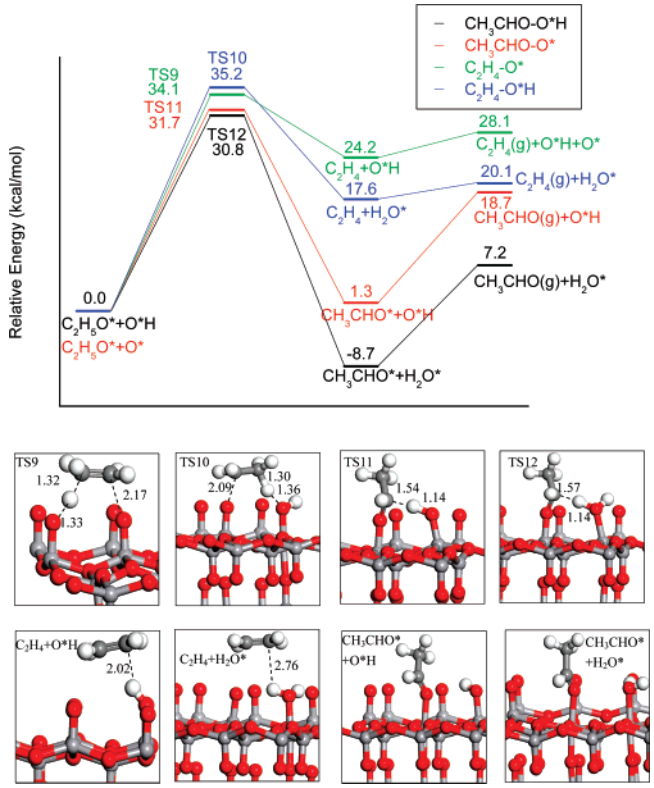

Figure 5. Reaction pathways of ethene and acetaldehyde formation through H abstraction from ethoxide by surface oxygen or a surface OH group at the O(1) site.

including O(1), O(2), and O(3) sites. After examining these three possible reaction pathways, we found that the H atom abstraction by the nearest O(1) atom is the most favorable pathway, with an energy barrier of 34.1 kcal/mol (Figure 5). The whole process is endothermic by 24.2 kcal/mol. In addition, the H atom may be abstracted by a nearby surface hydroxyl group O(1)-H to form ethene and water simultaneously. Since the formation and desorption of a water molecule may induce severe surface reconstruction, the pathway is explored by using a two-layer model of V_2O_5 (001). As shown in Figure 5, this process is endothermic by 17.6 kcal/mol with an energy barrier of 35.2 kcal/mol. Obviously, in the process of ethene formation, the O(1) and O(1)-H group have similar abilities to abstract an H atom from the ethoxide. In other words, after the first C−H activation step, all the O(1) sites on the surface are still active for the next step, H abstraction.

For an ethoxide at the O(2) site, the most feasible pathway of H abstraction utilizes a nearby O(2), with an energy barrier of 31.6 kcal/mol, which is 2.5 kcal/mol lower than that with an O(1) site (Figure 6). It is also found that the H atom of ethoxide at the O(2) site can be abstracted by O(3), with an energy barrier (32.7 kcal/mol) very similar to that by O(2) to form ethene, while the nearby O(1) site is the least feasible site for H abstraction, with a very high energy barrier (71.2 kcal/mol). The reason why the O(1) site is less feasible for H abstraction than O(2) is apparently due to the large distance (near 4.9 Å) between O(1) and O(2) on V_2O_5 (001) (Figure 1). Moreover, unlike O(1), the hydroxyl group at O(2) is found to be inert for ethene formation due to the high-energy barrier of 42.6 kcal/mol.

In summary, the O(1) site on the surface has secondary reactivity, which means that after the O(1) site accepts one H atom, forming an O(1)-H group in the first C−H bond activation step, it is still reactive for the ethene formation by breaking the C−H bond of ethoxide, while the O(2) site is blocked after the first step, C−H bond activation of ethane. But compared with that on the O(1) site, the ethoxide on the O(2) site more easily forms ethene through H abstraction by a nearby lattice O(2) atom. Considering that the energy cost for the methyl C−H bond breaking is the same regardless of the O(1) or O(2) site, the ease of ethene formation on the O(2) site is mainly due to the weaker O−C bond of ethoxide on the O(2) site, just as what we found in the case of propane ODH.[46]

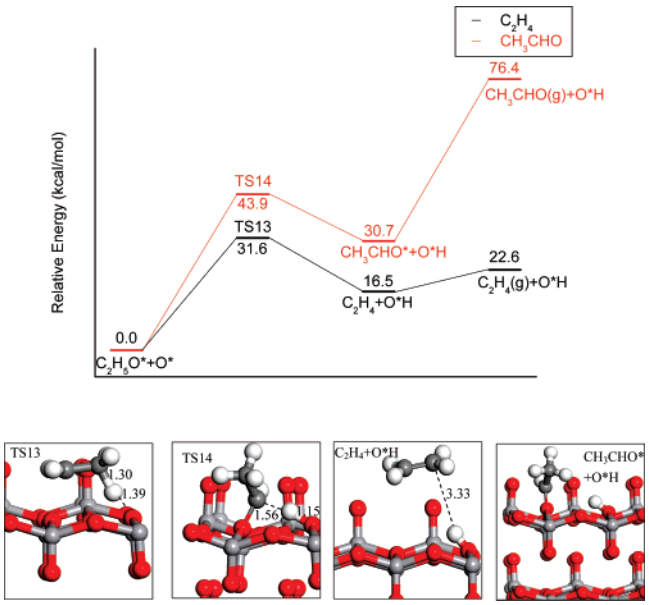

Figure 6. Reaction pathways of ethene and acetaldehyde formation through H abstraction from ethoxide by a surface O atom at the O(2) site.

3.4. Acetaldehyde Formation. Experimental studies indicated that ethene is the most abundant primary product of ethane ODH on VO_x/SiO_2,VO_x/Al_2O_3, and VO_x/ZrO_2,[2,54] and the other side-reaction products include acetaldehyde, CO_2, and CO. In order to obtain a better understanding of this process, we also explored the main side-reaction channel leading to acetaldehyde.

The possibility of the reaction taking place at the O(1) site is first investigated. Starting from the adsorbed ethoxide, a methylene H atom instead of a methyl hydrogen is abstracted by a nearby lattice O(1), yielding a surface CH_3CHO species (Figure 5). The energy barrier of this process is calculated to be 31.7 kcal/mol, and the reaction is endothermic by 1.3 kcal/mol. The energy cost for the desorption of the acetaldehyde molecule is 17.4 kcal/mol. Alternatively, the methylene hydrogen can transfer to a nearby hydroxyl group O(1)-H to produce a surface CH_3CHO species and a water molecule simultaneously, with an energy barrier of 30.8 kcal/mol. The process is exothermic by −8.7 kcal/mol, mainly due to the hydrogen bonding formed by the water molecule with a nearby O(1) (Figure 5). The desorption energy of acetaldehyde from the surface is 15.9 kcal/mol. It is noticed that the formation of acetaldehyde at the O(1) site is easier than the production of ethene, and the surface acetaldehyde species is sufficiently stable that it may undergo further oxidation to produce CO or CO_2. This could account for the low selectivity of the alkane ODH reaction.

For the reaction taking place at the O(2) site, the formation of acetaldehyde is very difficult, with a much higher energy barrier of 43.9 kcal/mol, and the process is endothermic by 30.7 kcal/mol. The overall energy profile is shown in Figure 6. In addition, if the acetaldehyde molecule desorbs from the surface, the structure of the catalyst falls apart, and the energy of desorption is as high as 45.7 kcal/mol. Therefore, we can conclude that the CH_3CHO species is unlikely to form at the O(2) site, which implies a higher selectivity of the O(2) site for the ethane ODH reaction.

3.5. Vanadium Reoxidation. Le Bars et al.[39] carried out a calorimetric experiment of ethane ODH on unsupported V_2O_5, which showed that O_2 is important in regenerating the vanadia surface and maintaining a high olefin yield. On the basis of our calculations, it is expected that water and acetaldehyde would desorb from the surface to create vacant O(1) sites easily. The subsequent reaction is the reoxidation of catalyst by the gas-phase oxygen. When the oxygen molecule in the gas phase attacks the unsaturated V sites, a stable molecular adsorption state is formed (as shown in Figure 7), with the adsorption energy of −6.7 kcal/mol. In the transition state (TS15), the distance between V and O is shortened to 1.66 Å (the normal V−O(1) bond length is 1.59 Å), which suggests that the V−O(1) bond is forming. At the same time, the activated O−O bond is almost broken, and the bond length is elongated from 1.28 Å to 1.78 Å. The other O atom of the activated oxygen molecule can transfer and bind with the nearby bare V site to form another V−O(1) bond. Finally, the initial V_2O_5(001) catalyst is regenerated, completing the catalytic cycle. The process of vanadium reoxidation is calculated to be exothermic by 86.9 kcal/mol, with a barrier of 35.1 kcal/mol. Obviously, the surface of catalyst can be reoxidated easily at high temperatures when it is exposed to O_2.

3.6. Discussion. On the basis of the results above, we summarized the overall energy profiles of the ethane ODH reaction in Figure 8. Generally, for the ODH reaction on V_2O_5, ethane shares many common features with propane. In the first step of C−H bond activation, the O(1) species on the surface is predicted to be more active than the O(2) site with the energy barrier lower by 3.5 kcal/mol. Similar to those in propane ODH reactions, the radical mechanism is preferred over O(1) for ethane C−H bond breaking, and the oxo insertion mechanism is preferred on O(2). As for the ethene formation by breaking the second C−H bond, the O(2) site is preferred over the O(1) site due to the weaker O−C bond of the ethoxide species on O(2). Also, the surface hydroxyl group O(1)-H has an ability similar to that of O(1) to abstract an H atom from ethoxide in ethene formation, while O(2)-H is inert in this step. By exploring the reaction channel toward the byproduct acetaldehyde, we found that the production of acetaldehyde from ethoxide is in fact easier than the production of ethene at the O(1) site (energy barrier of 30.8 kacl/mol vs 34.1 kcal/mol). Moreover, the acetaldehyde product is very stable on the surface compared with ethene (Figure 8) Therefore, the O(1) site is expected to have a low selectivity to ethene production, and the stable acetaldehyde on O(1) may be further oxidized to CO and CO_2. By contrast, the production of acetaldehyde over the O(2) site is more difficult, with an energy barrier of 12 kcal/mol higher than that of ethene production.

Overall, a clearer picture of the ethane ODH reaction over V_2O_5 emerged from our calculations. In agreement with the previous experimental and theoretical studies, the rate-limiting step of ethane ODH over V_2O_5 is the activation of the C−H bond. Both O(1) and O(2) species of the catalyst are active for C−H bond breaking, but the O(1) site is obviously more active. The higher activity of O(1) is attributed to two characteristics. First, the energy barrier for C−H bond activation at O(1) is lower than O(2). Second, the hydroxyl group O(1)-H has activity similar to that of O(1) in accepting H during ethene or acetaldehyde formation, which means that every O(1) on the surface provides two oxidative sites. However, the O(2) site has better selectivity to ethene due to both its lower energy barrier for ethene formation and its inertness for byproduct production.

From the discussion above, one can find that the calculated energy barrier of the rate-determining step of ethane ODH is 35.1 kcal/mol, which is about 7.8 kcal/mol higher than that of propane.[46] This result is consistent with the bond energy

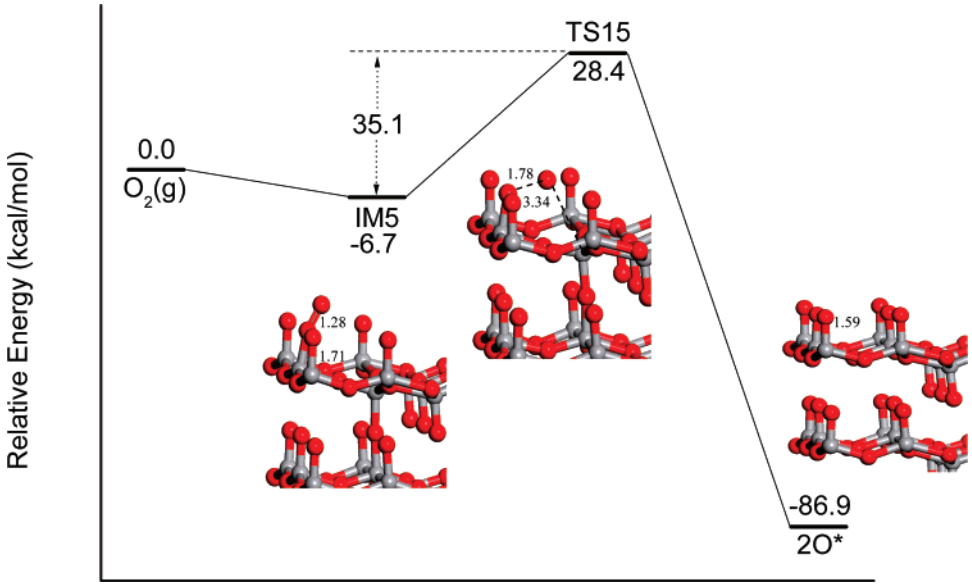

Figure 7. Reaction pathways and structural parameters for the transition states of the vanadium reoxidation step.

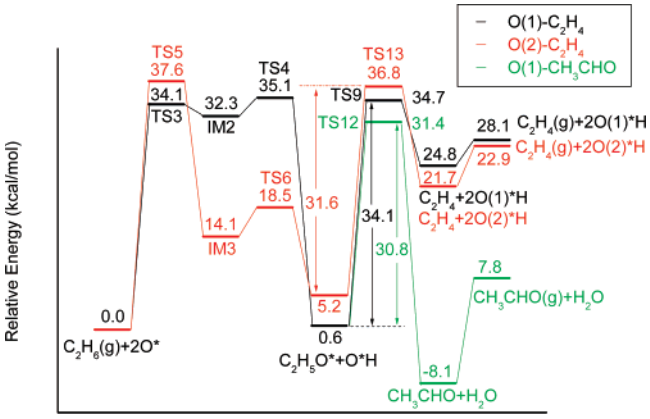

Figure 8. Lowest-energy pathways of the ethane ODH process occurred on O(1) and O(2), respectively.

difference between methyl and methylene C−H bonds (420 kJ/mol vs 401 kJ/mol). The DFT calculations on methane and propane ODH over Mo_3O_9 cluster also found a higher activation energy of C−H bond activation for methane than for propane.[42,43] However, the DFT results appear to conflict with the equivalence of the activation energies for ethane and propane ODH derived from the experimental kinetic data.[35,44] It is proposed that the stability of the intermediate species formed upon C−H bond activation may be the reason; that is, the higher stability of ethoxide than isopropoxide species could compensate for the difference in C−H bond energies in the transition state involved in C−H bond activation and lead to similar activation energies for the two alkane reactants.[35,44] However, this speculation is not supported by our calculations. On the contrary, the calculation shows that ethoxide species is in fact 1 kcal/mol less stable than isopropoxide on the surface.

Yet another puzzle exists in the comparison of ethane and propane ODH. According to the experimental results,[44] the rate of ethane ODH is much lower than that of propane while the activation energies are very similar. Therefore, it means that either the preexponential factor or the number of active sites must be much lower for ethane than for propane reactants. The lower preexponential factor reflects a larger negative entropy change upon transition state formation for ethane than for propane. By using the cluster model, the most feasible pathway of first step C−H bond activation of C_2H_6 and C_3H_8 at the O(1) site of Mo_3O_9 has been calculated to estimate the value of ΔS. As a result, the obtained ΔS for ethane C−H bond activation is −27.5 kcal/mol/K and that for propane is −35.9 kcal/mol/K at 873 K. So the activation entropy of propane ODH is more negative than that of ethane ODH rather than vise versa, which suggests that the entropy factor is unlikely to account for the much lower reaction rate of ethane ODH relative to propane. At first glance, it is also unlikely that the number of active sites for ethane ODH would differ from that of propane ODH since they share the same reaction mechanism in alkene formation. However, as indicated by the above calculations, the O(1) site bears very low selectivity for ethene production because of the competing process of acetaldehyde formation with a lower energy barrier. In addition, both O(1) and O(1)-H species are more active for acetaldehyde formation than for ethene formation (Figure 5). As for the propane ODH, the possible byproduct reaction routes were not examined in the previous study.[46] In order to compare with the ethane ODH, the possible side-reaction route starting from surface isopropoxide leading to acetone is evaluated here. The energy barrier required to form acetone is 28.6 kcal/mol, while that leading to propene is 28.2 kcal/mol. Therefore, on the O(1) site the formation of acetaldehyde is much more preferred to the formation of ethene while the propene production is competitive with acetone production. In other words, the O(1) site is much more effective, thereby contributing more to the rate of propane ODH than to ethane ODH. Although the C−H bond activation mechanisms in ethane and propane ODH are the same, the efficiency for alkene formation differs due to the different activity of lattice oxygens for side reactions. This may partly account for the rate difference of ethane and propane ODH although thorough understanding of the puzzle requires a more comprehensive study of all possible oxidation side reactions in alkane ODH. A detailed study of further oxidation reactions is undergoing in our group.

4. Conclusions

The mechanism of oxidative dehydrogenation reaction of ethane over a V_2O_5 (001) surface has been investigated for the first time by means of periodic DFT calculations. The main results are summarized below.

1. The ethane ODH over the V_2O_5 (001) surface follows a mechanism similar to that of propane. The first C−H bond

activation is the rate-limiting step of ethane ODH, leading to the ethoxide intermediate. C−H bond activation over the O(1) site through a radical mechanism is the most feasible route in this step, with an energy barrier of 35.1 kcal/mol. The energy barrier of C−H bond activation over the O(2) site through an oxo-insertion mechanism is 2.5 kcal/mol higher than that of O(1).

2. Ethene can be formed more easily at O(2) than at O(1) through the second C−H bond breaking from the ethoxide intermediate, with energy barriers of 31.6 kcal/mol and 34.1 kcal/mol, respectively. The surface hydroxyl group at the O(1) site has similar activity with O(1) for ethene formation.

3. As the byproduct of ethane ODH, acetaldehyde can be formed at the O(1) site via the dehydrogenation of ethoxide species, with a lower energy barrier than that of ethene formation (30.8 vs 34.1 kcal/mol). The surface hydroxyl group O(1)-H has similar activity for acetaldehyde production, while O(2) is inert for this side reaction. Acetaldehyde formation is an exothermic process, and its high stability on the surface may lead to further oxidation to CO or CO_2.

4. Vacant oxygen sites may be created after the desorption of water or acetaldehyde from the V_2O_5 (001) surface, and the O_2 in the gas phase may reoxidate the surface with an O−O bond breaking energy barrier of 35.1 kcal/mol, and the process is calculated to be exothermic by 86.9 kcal/mol.

5. The calculated energy barrier for the rate-limiting step of ethane ODH (35.1 kcal/mol) is higher than that of propane ODH (29.3 kcal/mol), and the ethoxide intermediate does not show a stabilization energy higher than that of isopropoxide, as proposed in former experimental studies.

6. The much lower ODH rate for ethane than for propane cannot be accounted for by the entropy effect that determines the preexponential factor. By considering the byproduct selectivity of various lattice oxygens, we propose that the much lower ODH rate of ethane relative to propane may be partly accounted for by the reduction of the number of active sites for ethane ODH due to the poor efficiency of the O(1) site for ethene formation.

Acknowledgment. This work was supported by the National Science Foundations of China (20433020, 20673024, 20633030) and the National Science Foundations of Shanghai Science and Technology Committee (05DZ22313, 04JC14016), National Major Basic Research Program of China (2003CB615807), Shanghai Education Committee (04SG05), Shanghai Leading Academic Discipline Project (B108). The Shanghai Supercomputing center and Fudan Computing center are thanked for computing time.

References and Notes

(1) Bettahar, M. M.; Costentin, G.; Lavalley, J. C. *Appl. Catal. A* **1996**, *145*, 1.
(2) Oyama, S. T.; Middlebrook, A. M.; Somorjai, G. A. *J. Phys. Chem.* **1990**, *94*, 5029.
(3) Oyama, S. T. *J. Catal.* **1991**, *128*, 210.
(4) Zhao, Z.; Yamada, Y.; Teng, Y.; Ueda, A.; Nakagawa, K.; Kobayashi, T. *J. Catal.* **2000**, *190*, 215.
(5) Kung, H. H. *Adv. Catal.* **1994**, *40*, 1.
(6) Mamedov, E. A.; Cortes-Corberan, V. *Appl. Catal. A* **1995**, *127*, 1.
(7) Hong, S. S.; Moffat, J. B. *Appl. Catal. A* **1994**, *109*, 117.
(8) Chen, K. D.; Bell, A. T.; Iglesia, E. *J. Phys. Chem. B* **2000**, *104*, 1292.
(9) Xie, S. B.; Chen, K. D.; Bell, A. T.; Iglesia, E. *J. Phys. Chem. B* **2000**, *104*, 10059.
(10) Chen, K. D.; Iglesia, E.; Bell, A. T. *J. Phys. Chem. B* **2001**, *105*, 646.
(11) Chen, K. D.; Bell, A. T.; Iglesia, E. *J. Catal.* **2002**, *209*, 35.
(12) Chen, K. D.; Xie, S. B.; Iglesia, E.; Bell, A. T. *J. Catal.* **2000**, *189*, 421.
(13) Chen, K. D.; Iglesia, E.; Bell, A. T. *J. Catal.* **2000**, *192*, 197.
(14) Chen, K. D.; Khodakov, A.; Yang, J.; Bell, A. T.; Iglesia, E. *J. Catal.* **1999**, *186*, 325.
(15) Albonetti, S.; Cavani, F.; Trifirò, F. *Catal. Rev.-Sci. Eng.* **1996**, *38*, 413.
(16) Cadus, L. E.; Gomez, M. F.; Abello, M. C. *Catal. Lett.* **1997**, *43*, 229.
(17) Centi, G. *Appl. Catal. A* **1996**, *147*, 267.
(18) Miki, J.; Osada, Y.; Konoshi, T.; Tachibana, Y.; Shikada, T. *Appl. Catal. A* **1996**, *137*, 93.
(19) Grzybowska, B. *J. Catal.* **1997**, *68*, 423.
(20) Busca, G. *Catal. Today.* **1995**, *24*, 307.
(21) Michalakos, P.; Kung, M. C.; Jahan, I.; Kung, H. H. *J. Catal.* **1993**, *140*, 226.
(22) Sananes-Schulz, M. T.; Tuel, A.; Hutchings, G. J.; Volta, J. C. *J. Catal.* **1997**, *166*, 388.
(23) Gao, X.; Ruiz, P.; Xin, Q.; Guo, X.; Delmon, B. *J. Catal.* **1995**, *148*, 56.
(24) Grasselli, R. K. *Catal. Today* **1999**, *45*, 141.
(25) Chaar, M. A.; Patel, D.; Kung, H. H. *J. Catal.* **1988**, *109*, 463.
(26) Corma, A.; Lopez, Nieto, J. M.; Paredes, N. *J. Catal.* **1993**, *144*, 425.
(27) Hardcastle, F. D.; Wachs, I. E. *J. Mol. Catal.* **1988**, *46*, 173.
(28) Deo, G.; Wachs, I. E.; Haber, *J. Crit. Rev. Surf. Chem.* **1994**, *4* (3/4), 141.
(29) Wachs, I. E.; Wechuysen, B. M. *Appl. Catal. A* **1997**, *157*, 67.
(30) Eon, J. G.; Olier, R.; Volta, *J. Catal.* **1994**, *145*, 318.
(31) Balsko, T.; Lopea Nieto, J. M. *Appl. Catal. A* **1997**, *157*, 117.
(32) Khodakov, A.; Olthof, B.; Bell, A. T.; Iglesia, E. *J. Catal.* **1999**, *181*, 205.
(33) Khodakov, A.; Yang, J.; Su, S.; Iglesia, E.; Bell, A. T. *J. Catal.* **1998**, *177*, 343.
(34) Kondratenko, E. V.; Baerns, M. *Appl. Catal. A* **2001**, *222*, 133.
(35) Argyle, M. D.; Chen, K. D.; Iglesia, E.; Bell, A. T. *J. Catal.* **2002**, *208*, 139.
(36) Mars, P.; van Krevelen, D. W. *Chem. Eng. Sci., Special Suppl.* **1954**, *3*, 41.
(37) Creaser, D.; Andersson, B.; Hudgins, R. R.; Silveston, P. L. *Appl. Catal. A* **1999**, *187*, 147.
(38) Mamedov, E. A.; Cortés, Corberán, V. *Appl. Catal. A* **1995**, *127*, 1.
(39) Le Bars, J.; Vedrine, J. C.; Aurous, J, A.; Trautmann, S.; Baerns, M. *Appl. Catal., A* **1992**, *88*, 179.
(40) Haber, J.; Witko, M. *J. Catal.* **2003**, *216*, 416.
(41) Grzybowska-Swierkosz, B. *Top. Catal.* **2000**, *11/12*, 23.
(42) Fu, G.; Xu, X.; Lu, X.; Wan, H. *J. Am. Chem. Soc.* **2005**, *127*, 3989.
(43) Fu, G.; Xu, X.; Lu, X.; Wan, H. *J. Phys. Chem. B* **2005**, *109*, 6416.
(44) Heracleous, E.; Machli, M.; Lemonidou, A. A.; Vasalos, I. A. *J. Mol. Catal. A* **2005**, *232*, 29.
(45) Redfern, P. C.; Zapol, P.; Sternberg, M.; Adiga, S. P.; Zygmunt, S. A.; Curtiss, L. A. *J. Phys. Chem. B* **2006**, *110* 8363.
(46) Fu, H.; Liu, Z.-P.; Li, Z.-H.; Wang, W.-N.; Fan, K.-N. *J. Am. Chem. Soc.* **2006**, *128*, 11114.
(47) Junquera, J.; Paz, O.; Sanchez-Portal, D.; Artacho, E. *Phys. Rev. B* **2001**, *64*, 235111.
(48) Troullier, N.; Martins, J. L. *Phys. Rev. B* **1991**, *43*, 1993.
(49) Perdew, J. P.; Burke, K.; Ernzerhof, M. *Phys. Rev. Lett.* **1996**, *77*, 3865.
(50) http://www.netlib.Org/scalapack/scalapack_home.html.
(51) Liu, Z. P.; Jenkins, S. J.; King, D. A. *J. Am. Chem. Soc.* **2004**, *126*, 10746.
(52) Liu, Z. P.; Hu, P. *J. Am. Chem. Soc.* **2003**, *125*, 1958.
(53) Martin, G. A.; Mirodatos, C. *Fuel Process. Technol.* **1995**, *42*, 179.
(54) Argyle, M. D.; Chen, K. D.; Bell, A. T.; Iglesia, E. *J. Phys. Chem. B* **2002**, *106*, 5421.